

Characteristics and Performances of Biplane Airfoil



MECHANICAL AEROSPACE ENGINEERING

AEROSPACE LABORATORY - WINDTUNNEL LAB

Professor Gamero-Castaño

Submitted By:

Jin Mok

Date: 12/09/13

Table of Contents

Abstract.....	3
Introduction.....	4
Experiment Description.....	6
Data and Results.....	8
Interpretation of Results.....	12
Conclusion.....	15
References and Acknowledgement.....	16
Appendices.....	16
Sample Calculations.....	17

Abstract

From the first flight of Wright Brothers in 1903, it was an event that rattled the world. After their first flight, the competition for superior design airplane became exponentially demanding as military perceived that the air superiority as decisive advantage in World War I and II. In the early aspects of aircraft performance of bi-planes, bi-planes had dominance over monoplane from the structural advantage. The design parameters that should be considered initially for bi-planes are 'gap', 'span ratio', 'stagger' and 'decalage'. The experiment is based on relative position of the upper and lower wing located to identify aerodynamic characteristics of the bi-plane. In this experiment, two RAF-15 airfoils were 3D printed with gap of 85% chord length of the airfoil. The collected the aerodynamic properties were compared along with staggered position from +100% to -100% of chord length in increments of $\pm 25\%$ also having 0° decalage. Also relative loadings on the upper and lower airfoils will be calculated to dimensionless parameters to see the aerodynamic characteristics. The Reynolds number that this experiment was tested was 60,552. The comparison of staggered positions of the wings will be compared to experiments shown in NACA report 330, 70, 458, where correlation of staggered wings influence coefficient of lift, drag, moment and L/D. The gap was at 0.85 chord length between the wings and we were able to compare the patterns in aerodynamic properties between staggered bi-plane wings and 85% chord length was optimal to be influenced by wall effect.

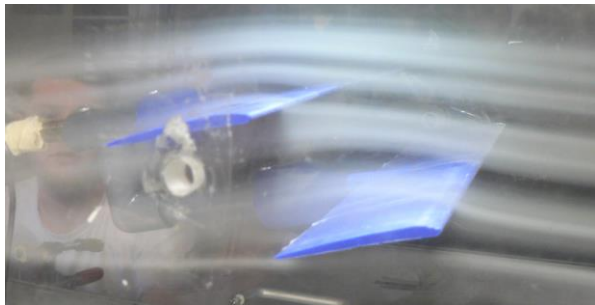


Figure 1.1: Flow visualization of negatively staggered bi-plane airfoil set up

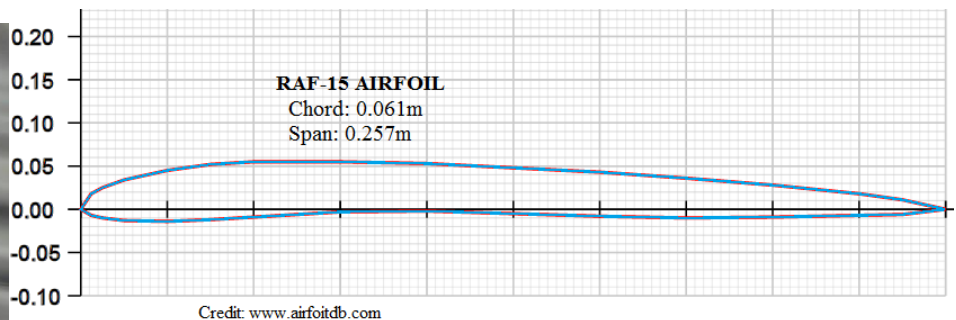


Figure 1.2: Airfoil geometry with test chord and span length

1. Introduction

1.1. Purpose and Objective

The purpose and objective of this experiment was to examine the difference between the aerodynamic properties of single airfoil and staggering two airfoils for bi-plane design. The objective is to determine the staggered percentage to optimize coefficient of lift, drag and moment as well as to understand how the airflow from staggered position would influence the characteristics of upper and lower airfoils in relation to single airfoil. The objective will be to determine the differential between the staggered positions of the airfoils and compare and calculate the lift coefficient of two airfoil set up that was held constant span ratio, gap and decalage while varying angle and staggered position.

1.2. Brief Review of Basic Problem

The rational assumption of two airfoils producing double the lift is absolutely imprecise. Thus, the problem is to determine the optimal staggered ratio that would yield ideal lift-to-drag ratio, as well as lift and drag coefficients. One must consider the airflow from front airfoil's interaction with the one behind due to difference in pressure and relative velocity. By varying the angle of attack, the velocity and pressure difference between frontal airfoil and airfoil behind can be explained through Prandtl's interference factor and the Venturi effect. Also, in theory, bi-plane with the same area upper and lower wing should permit half the induced drag to that of same wing span, but due to mutual interference about 30% is achieved. From this experiment, we would also see how much induced drag percentage bi-plane airfoils will yield in comparison to monoplane airfoil. Lastly, from this experiment the relationship between aerodynamic characteristics and relative staggered position of the airfoils will be determined.

1.3. Theoretical Background

The issue with the bi-plane design from early 1900's was that bi-plane did not generate enough lift as it was expected with two airfoils instead of monoplane also excessive drag produced. Although monoplanes were available, structural properties were not able to withstand the structural loading that was produced during flight. Thus, bi-plane had structural advantage over monoplanes, whereas bi-planes had more drag yielded by the mounts, struts and strings to hold structural integrity. Aerodynamic properties of the bi-plane can be analyzed through dimensionless parameters such as coefficient of lift, drag and moment. $C_L = \text{Lift}/\rho V^2 S$, similarly as $C_D = \text{Drag}/\rho V^2 S$ as well as the moment, which will be $C_m = \text{Moment}/\rho V^2 c^2$. Theoretically, there are two utmost factors that determine the complex bi-plane theory.

First is the mutual interferences of the vortex system of each wing increases downwash and induced drag. Secondly, the additional downwash and induced drag is created due to curvature of the airflow over the airfoil, which is determined by gap-to-chord ratio. Such that the effects of upfront airfoil will influence the other. One example of importance of gap-to-ratio is that gap between the airfoils can be considered Venturi effect which is in function of angles of attack, and percent staggered. In comparison with the monoplanes, the bi-planes with 0 staggered will have same location for center of pressure, however, higher percentage staggered of the airfoils, center of pressure will move towards the leading edge. It is important to locate the center of pressure due to the fact that the lift generated at center of pressure will be substantially located away from center of gravity. Thus, it is important to indicate that center of pressure would vary with lift coefficient for cambered airfoil RAF-15 and it will be used as an alternate by calculating lift and moment coefficient to verify the integrity of the data collected. Also, by calculating the stall characteristic of both single airfoil and both airfoils for bi-plane will be computed and graphed. Also, by using Max Michael Munk's equivalent monoplane equations for bi-planes will be utilized to compare the upper and lower airfoils. The relationships of airflow on upper and lower airfoil in respect to the bi-plane airfoil characteristics are discussed with experimental data and analysis done by Walter S. Diehl, Report No. 458: Relative Loading on Biplane wings.

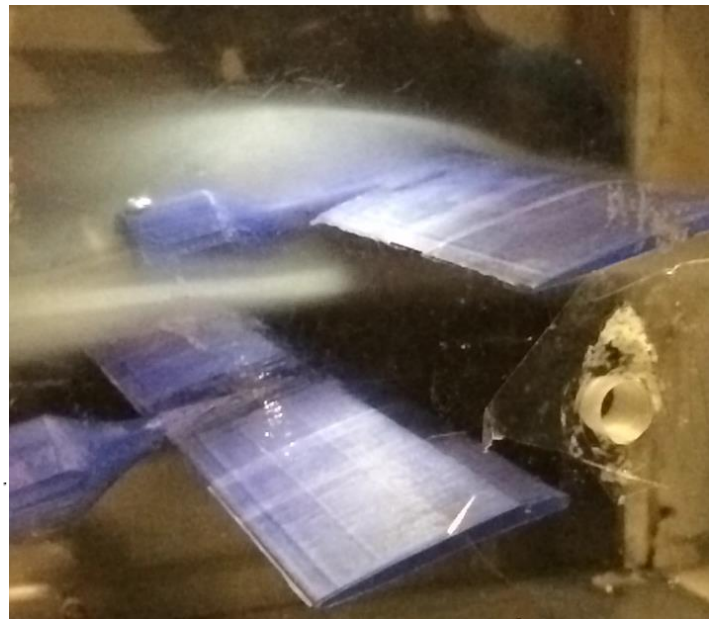
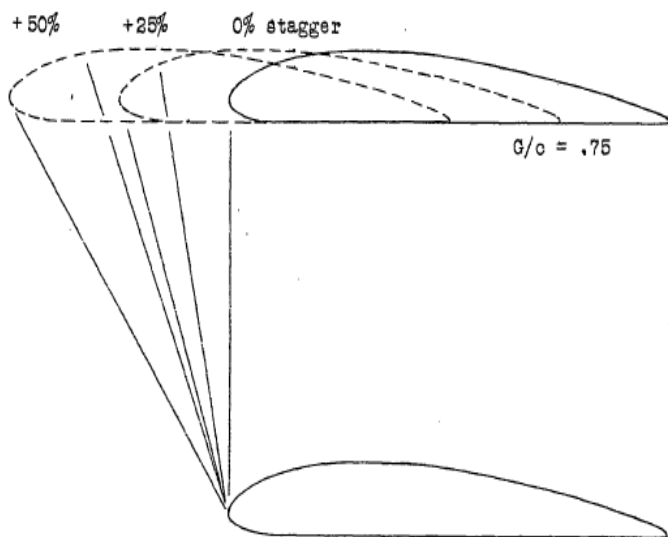


Figure 2.1:Credit to NACA report 330

1.4. Outline of Report/Scope

This report will be based on the fundamental knowledge of 2 dimensional airfoil aerodynamic coefficients for viscous and inviscid flow and brief calculations of 3 dimensional properties of the airfoils using Munk's methodology. This experiment determines the lift, drag, moment and aerodynamic center of single and two RAF-15 airfoil to show the effect of percent staggered on such parameters. The correlation of aerodynamic properties between the single airfoil and the bi-plane airfoil (percent staggered) would pristinely show the optimal airfoil design characteristics that will be compared with NACA 70 and 330's experimental values.

2. Experiment Description

2.1. Description of Instruments Used

The experiment utilized the same wind tunnel where test section is 30 cm wide with maximum velocity of 35 m/s. However, due to wall effects, this experiment was limited to gap 5.185 cm between two wings. Also, the forces and torque measurements were taken by ATI NANO17 sensor and strain-gauge sting balance which sends signal to LabVIEW program. These two instruments gives precise readings of forces and torques generated and the precision values is shown in **table 2.1**. Three different weights were used for calibration also scales, calipers, and inclinometer were used to calculate the forces and torques incorporated with the sting balance. The airfoils that were used have been attached by various pipes that were premeasured to position the airfoils staggered accordingly. The static pressure tap was used to measure the velocity inside the tunnel. The airfoils were 3D printed and various pipe length were used to stagger the airfoils relative to each other in increments 25% chord length (Fig 2.1). Also, we utilized the fog machine at the maximum and minimum staggered position in order to visualize how flow behaves under different conditions.

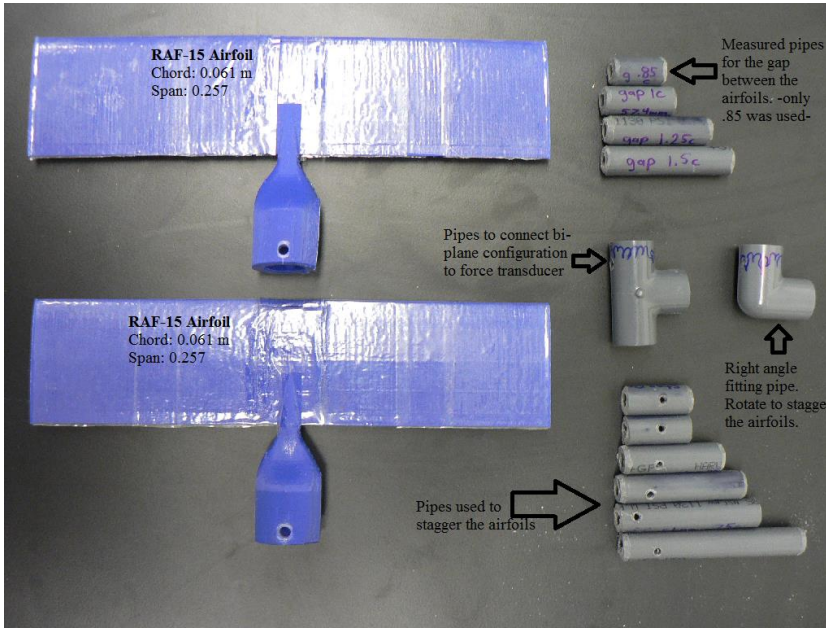


Figure 2.2: Equipments used for experiment

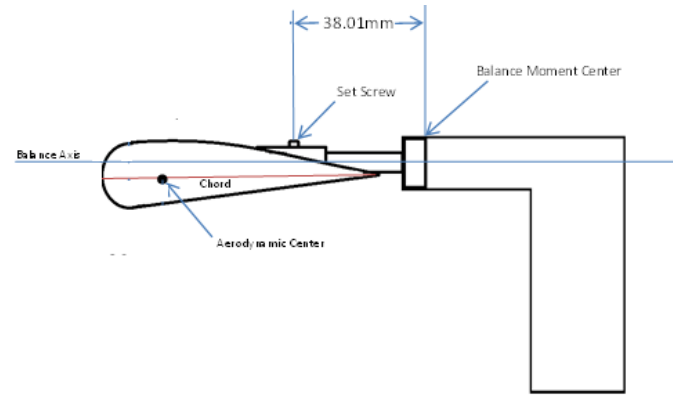


Figure 2.3: Distance from set screw to force balance

Measurement Device	Precision
Length (m)	0.0050
Pressure Transducers (Pa)	0.5600
Balance Precision Force (N)	0.0028
Balance Precision Torque (Nm)	1.6E-05

Table 2.1: Precision of devices used.

2.2. Configuration of the Experiments

Every experiment started with the calibration of the force balance. Also, calibration was needed at every increments of angle change. First, to calibrate the force balance, it was required that every buck values were measured and incorporated as the wind tunnel was turned off. During the first lab hours, we experimented with only one RAF-15 airfoil. 10 different angles of attack contributed to measurements at 15 m/s from -4° to 14° in 2° increments. After 15 m/s , the airspeed increased to value of 25 m/s and the angles of attack were from -4° to 6° in 2° increments, and did not go beyond 6° due to maximum load that the force balance can withstand. As for the two airfoils attached at 5.185 cm gap in between, which is the 85% chord gap, and bucked at every angles of attack; however, now the measurements gathered were from relative position of percentage staggered of two airfoils. The bi-plane experiment did not exceed 15 m/s to not exceed the force limitation of the force balance. The maximum and minimum positions of the two airfoils were at $\pm 100\%$ chord length and staggered in increments of $\pm 25\%$ for every

measurement. Measurements with correction from wall effect and without F_x , F_z and T_y was used to plot L/D , C_L , C_D as well as C_m versus α . Also, fog machine were used after the data collection. The extraneous forces produced by the pipe that connects the airfoils together were calculated after the data was gathered for the staggered airfoils. After data collection of the total forces with both airfoils, we took the airfoils off and collected the forces and torque generated by the pipes with holes for bolts covered-

3. Data/Results

3.1. Wall Effects

To minimize the error from the wall/ground effect, we have used the previous calculation from the lab to reduce forces caused by wall effect. The correction is shown in the appendix.

3.2. Plots of C_L , C_D , and C_m Single Airfoil at 15 m/s and 25 m/s

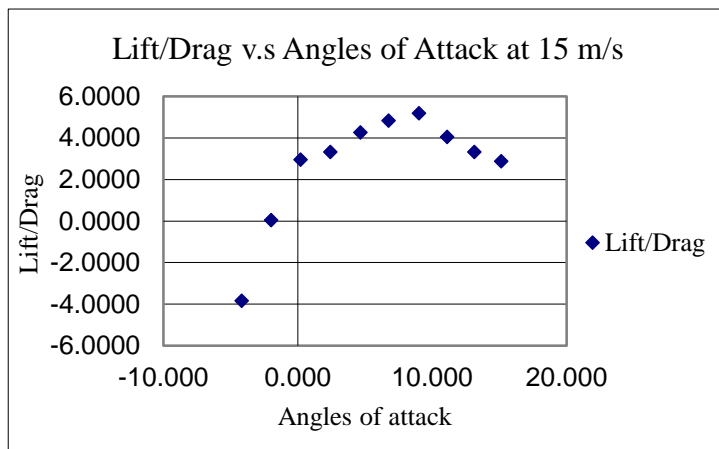


Figure 3.1 L/D v.s Angle of Attack at 15m/s

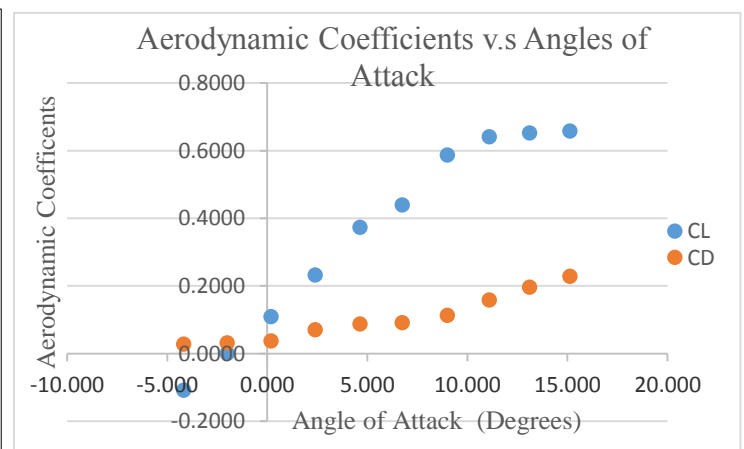


Fig 3.2 L/D v.s Angle of Attack at 15 m/s

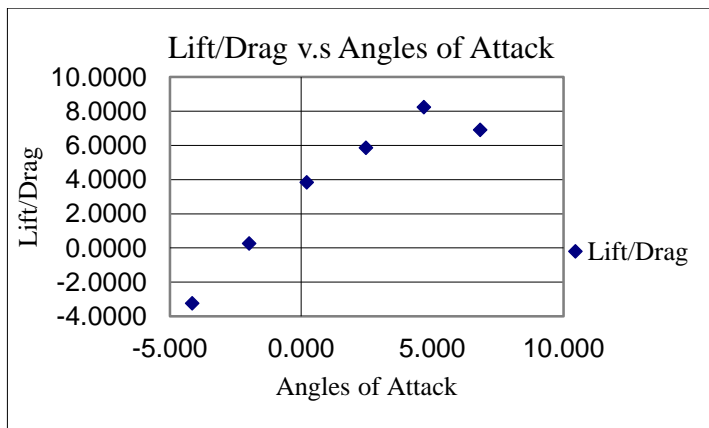


Figure 3.3 L/D v.s Angle of Attack at 25 m/s

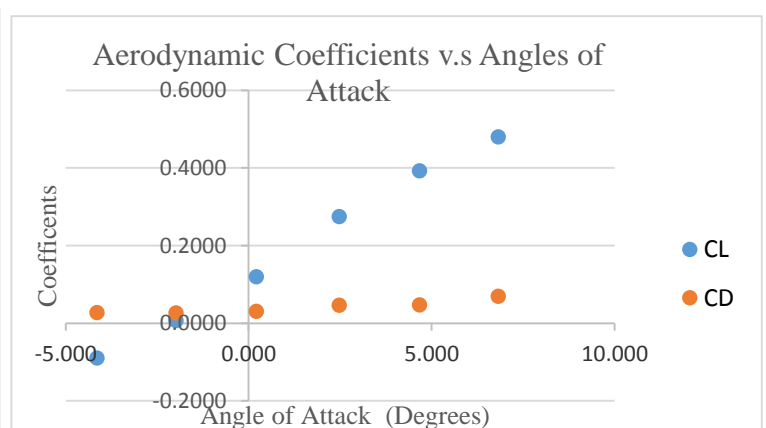
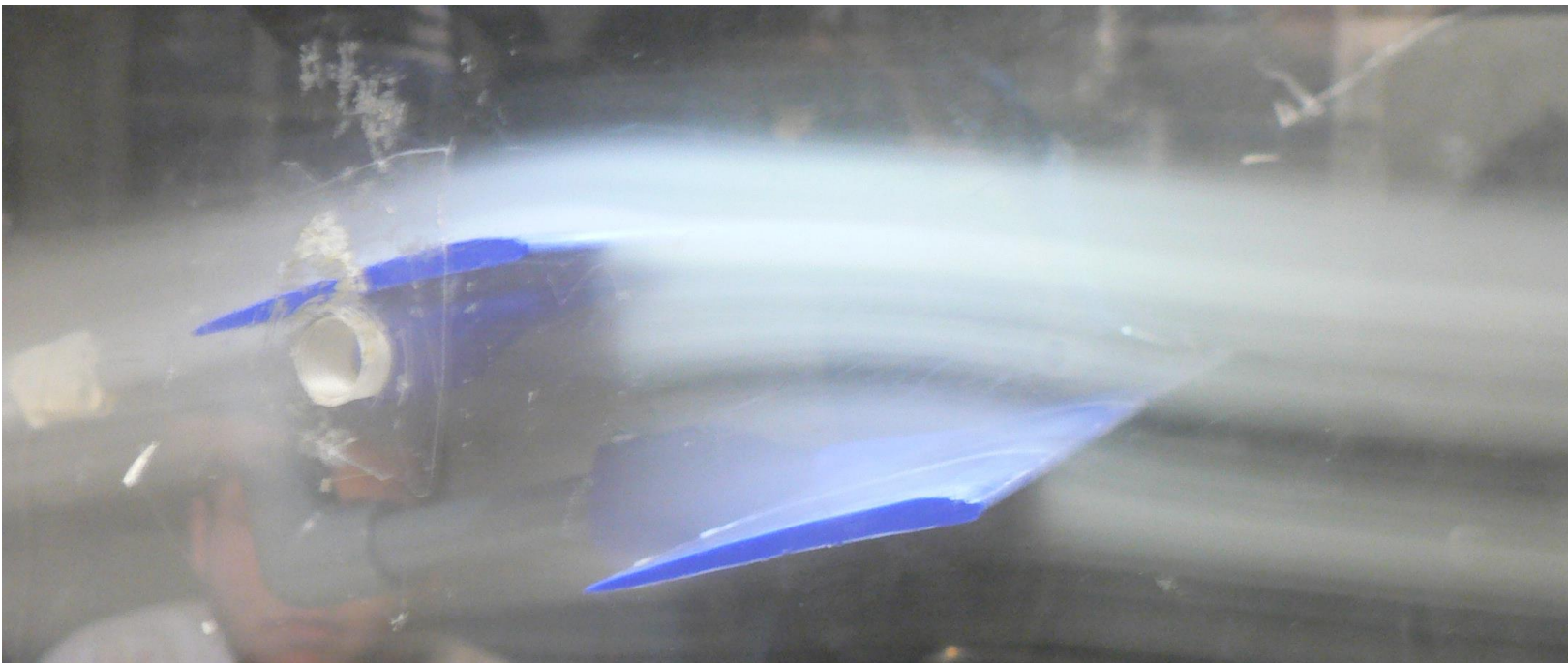
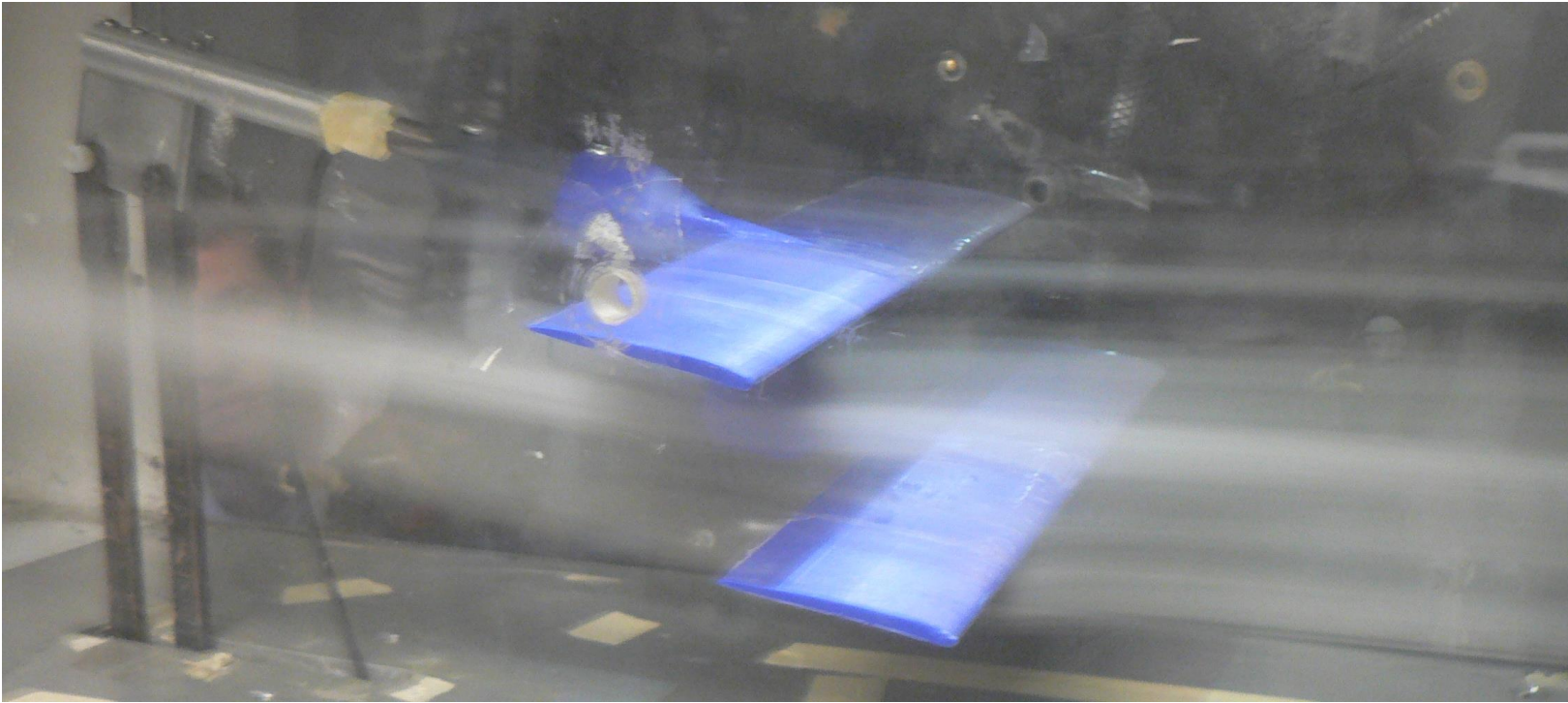


Fig 3.4 C_L , C_D , C_m v.s Angle of Attack 25 m/s

The single airfoil aerodynamic characteristics were plotted and stall characteristics can be concluded from these. The stall angle were assumed to be around 12° by looking at the trend; however this is only for single airfoil at velocity 15 m/s and 25 m/s.



3.3. Aerodynamic Characteristic Plot v.s Angle of Attack for Two Airfoils

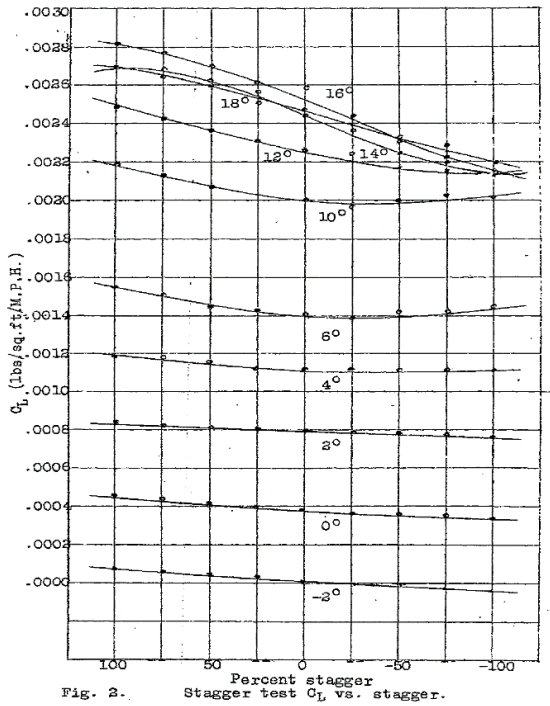


Figure 3.5: Result of CL v.s percent stagger from NACA 330 of Clark-Y airfoil.

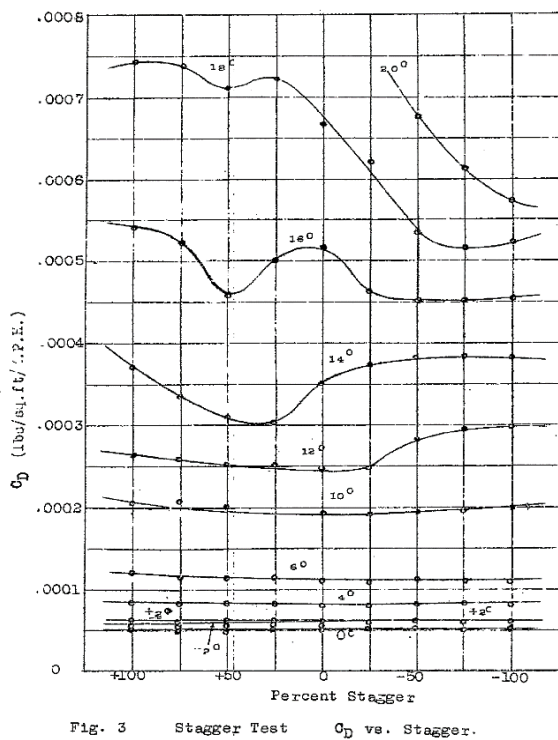


Figure 3.7: CL vs % staggered NACA 330 Clark - Y

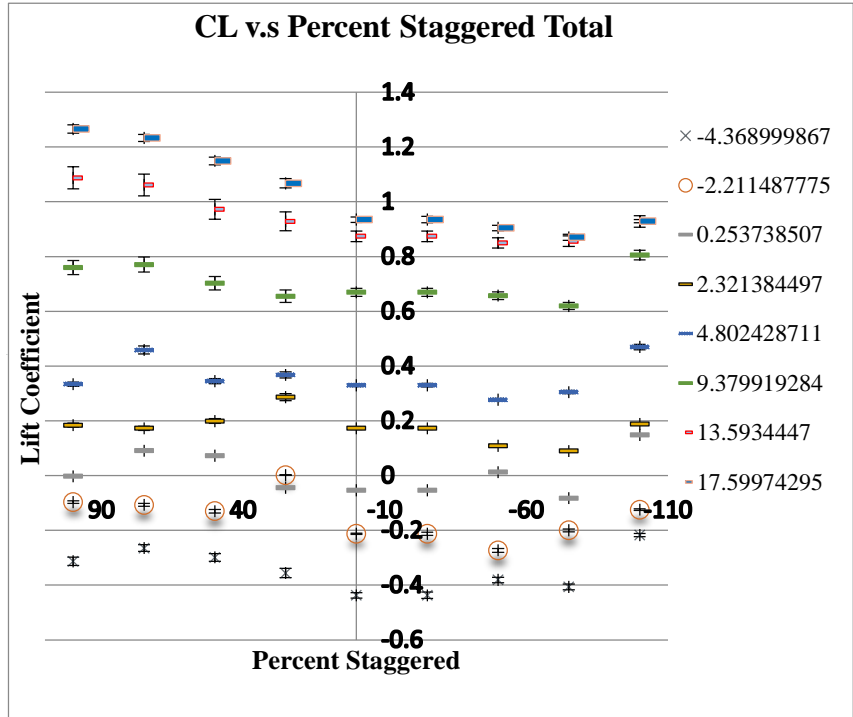


Figure 3.6: Lift coefficient v.s percent staggered in different angles of attack.

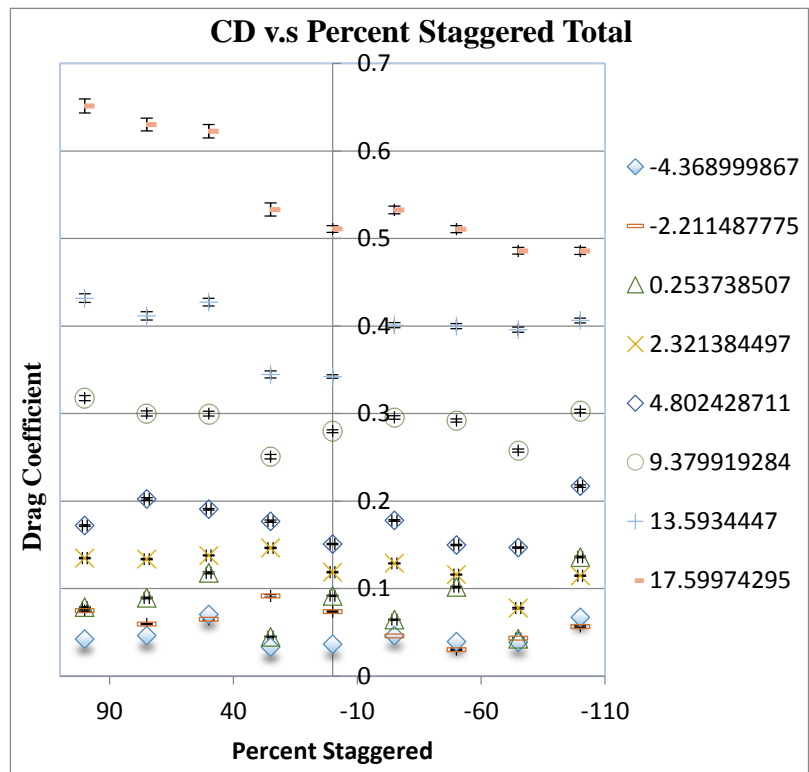


Figure 3.8: Drag coefficient v.s percent staggered in different angles of attack.

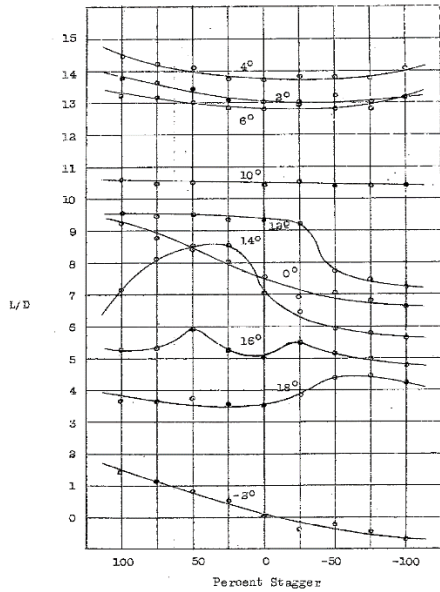


Figure 3.9: Result of lift/drag v.s percent stagger

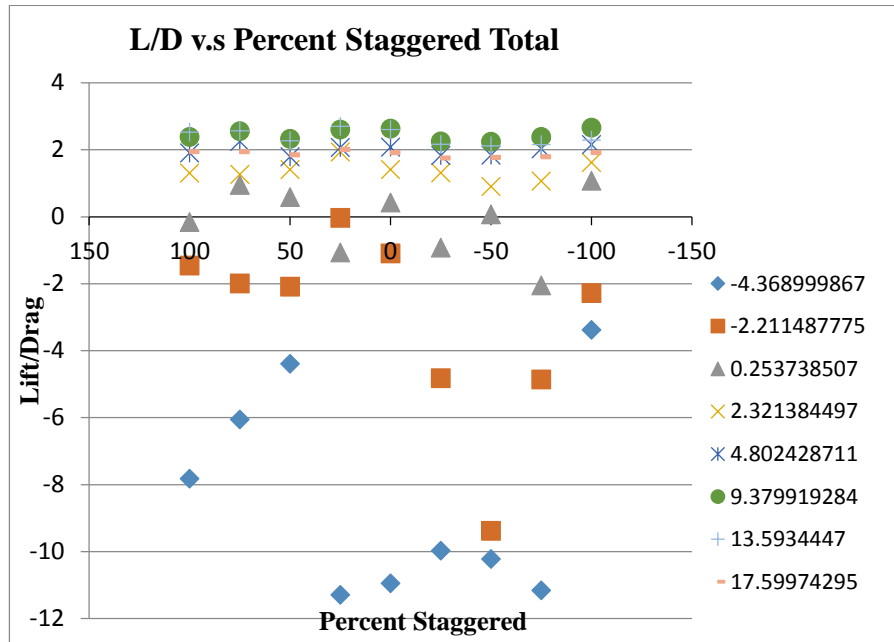


Figure 3.10: Lift/drag v.s percent staggered at different angles of attack.

The graphs shown compare the trend between the graphs from NACA reports 330 and the calculated data from the experiment. The graphs that are plotted from our experiment did not subtract the value of the pipes used; plotted values are the actual values of the bi-plane set up. The “Total” defines the values determined by the bi-plane set up without subtracting data collected from the pipe configurations.

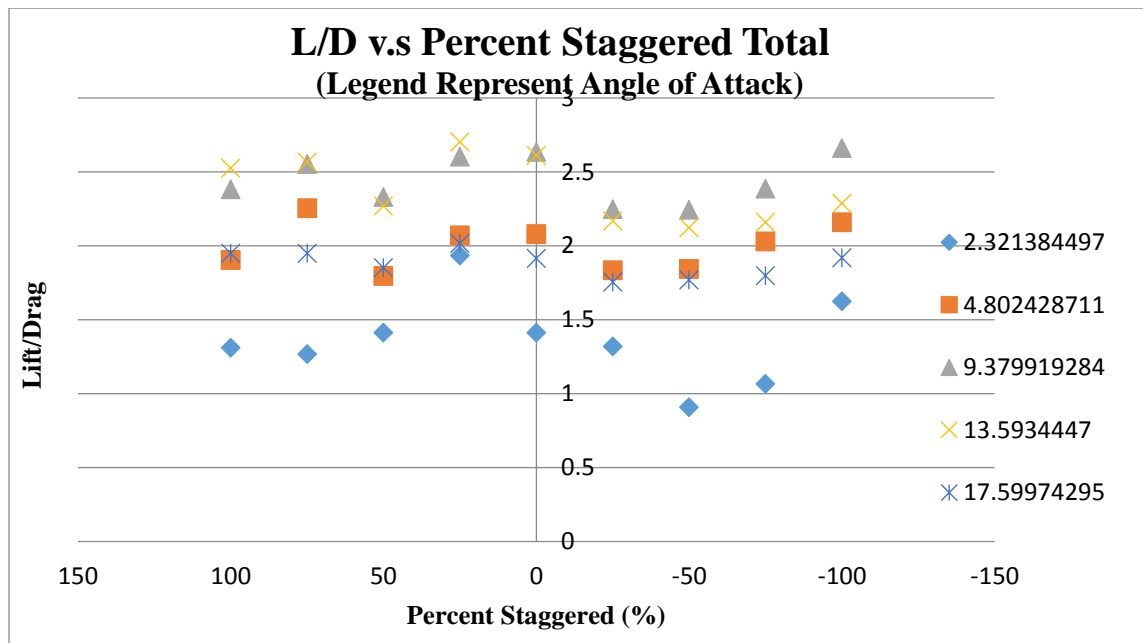


Table 3.11: L/D v.s percent staggered for angles of attack above 2 degrees.

4. Interpretation of Results

4.1. Position analysis of the configuration

The major difference in the aerodynamic characteristics of the bi-plane configuration is the relative position that the upper and lower airfoil is positioned respectively. The relative positions of the airfoils were used to determine lift and drag coefficient. By having fixed gap length, the aerodynamic qualities were compared to every relative position with similar parameters such as angles of attack and the velocity. The configuration of the airfoils attached to the pipes and the piping would yield extraneous forces, so calculations were made so that the data would subtract the extraneous forces caused by the airfoil attachment. However, the data collected for the configuration of the pipes that are used to connect the airfoils together cannot be concluded to be neither exact nor similar. Thus, the attempt to calculate precise airfoil aerodynamic properties yielded much more error and caused spikes in our graphs and data yielded from the airfoils without pipe configuration was not used for this analysis.



Figure 4.1: Attempts to calculate the extraneous forces by this configuration.

100% and -100%, the stall characteristic can be concluded from the lift coefficient and angles of attack. When the airfoils are positively staggered, the stall angle seems to be higher from the graphical trend, however, the negatively staggered airfoils have maximum lift coefficient at angle around 12 to 13 degrees. The comparison between the lift coefficient of NACA report and our experiment is shown from figure 3.5 and figure 3.6. The three main data that are critical to this analysis are maximum, minimum and no stagger.

4.2. Stall Characteristic

The stall characteristic of single airfoil is clearly shown by the figure 3.2, however, to determine the stall characteristics of the bi-plane set up is much more intricate. The stall characteristic of the positive staggered position cannot be determined with the data collected; however, the stall angle of negative staggered position can be determined by the graphical representation. The results yielded that the stall angle decreases with more negative staggered position. This is supported by the fact that the flow over the top of the front airfoil perturbs and the upper airfoil will not have smooth incoming airflow. In contrast, the positively staggered airfoil would have higher stall angle with the Venturi effect that can be applied, the airflow on the bottom surface of front upper airfoil will direct the airflow to be nearly aligned with the bottom airfoil at staggered position. Thus, generating flow that the lower airfoil will favor unlike the negative staggered.

4.3. Comparison with NACA report

As represented in the data, multiple positions that was tested for the bi-plane set up yielded similar data for lift and drag coefficient, which are shown from the figure 3.7, figure 3.8, figure 3.9 and 3.10. These figures compare the experimental data done at Engineering Gateway with open-loop with the data done by NACA experimental values. Even though the values calculated are not within the range of one another, the trend that these data follows is the purpose of the experiment. The trend between the lift and drag coefficient is what is most important due to the fact that even with the different parameters, the trend shows that the experiment was done correctly.

4.4. Relative Loading of the Airfoils

The calculation of relative loading of the airfoils are cruel because the incoming airflow is uniform, however, the effective angle of attack changes with respect to the airfoil that is in the front. Because the flow changes the angle of attack for the other airfoil, the loading on the upper and lower airfoils will be too complex to determine. The methods that the Munk and Prandtl used to solve this problem resulted to compare much more parameters. Also, one of the methodologies that were used by Prandtl was to compare the bi-plane equivalent to a monoplane. It used equations that relate gap-to-span ratio and the Munk's span factor in order to compensate for the Venturi effect and downwash generated by each wing relative to the other. This report will not calculate the relative loading of the upper and lower airfoils, but it will introduce the methodology of calculating loading of upper and lower airfoils.

4.5. Effects of Stagger Percentage

The graphs that are tabulated for lift, drag and L/D versus percent staggered gives clear idea of how these bi-plane airfoils have performed. As the lift and drag coefficient follows the general trend of NACA report, the L/D characteristic does not mirror NACA report. But, the only angles with positive L/D values are for angles of attack more than 0 and it is determined by figure 3.10. Comparing the lift coefficient at 100% and -100% staggered for angles of attack above 10 degrees tends to have higher CL at positive staggered but for the lower angles of attack below 10 degrees negatively staggered position has higher lift coefficient. For drag coefficients, the change is more drastic at higher angles of attack and the pattern of increasing or decreasing drag coefficient at range of angles of attack and it is shown by table 4.1. Change in lift coefficient is shown by table 4.2. Drag polar is also tabulated.

AoA	100	Cd	-100
-4.369	0.042527	<	0.067078
-2.21149	0.075079	>	0.056788
0.253739	0.078812	<	0.136044
2.321384	0.134847	>	0.114769
4.802429	0.171999	<	0.217134
9.379919	0.317686	>	0.30286
13.59344	0.431863	>	0.406359
17.59974	0.651422	>	0.485878

Table 4.1: Change in drag coefficient at maximum positions

AoA	100	Cl	-100
-4.369	-0.33281	<	-0.22635
-2.21149	-0.10911	<	-0.12926
0.253739	-0.01204	<	0.146869
2.321384	0.176662	<	0.186587
4.802429	0.327612	<	0.469083
9.379919	0.756905	<	0.805985
13.59344	1.090842	>	0.929122
17.59974	1.269935	>	0.932714

Table 4.2: Change in lift coefficient at maximum positions

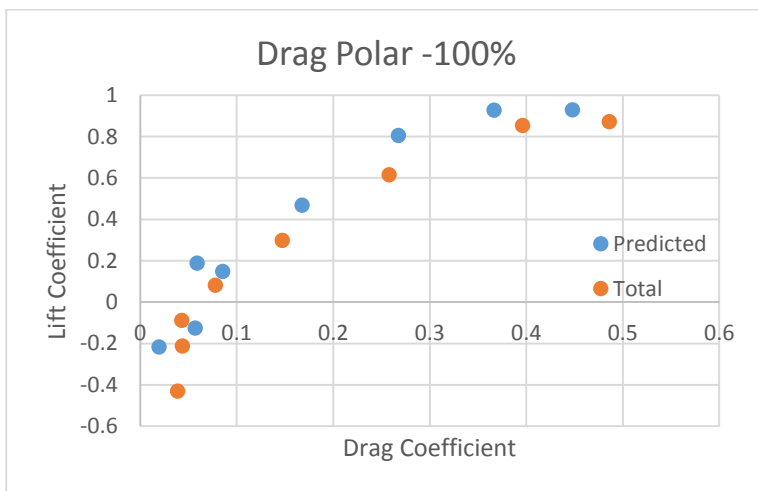


Table 4.3: Drag polar for -100%

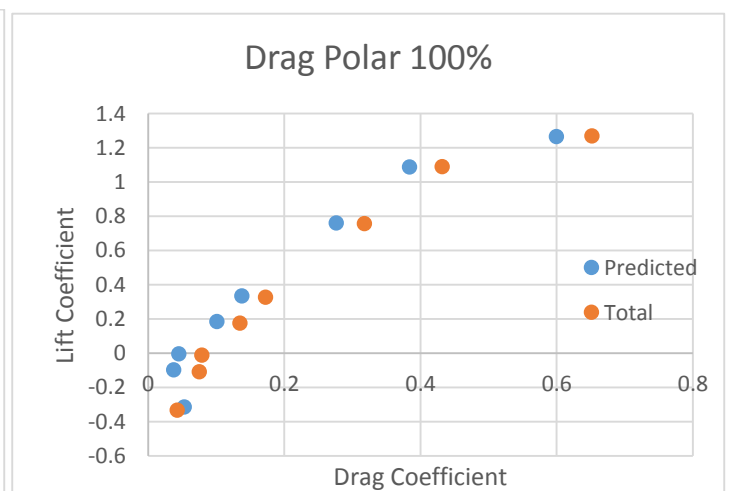


Table 4.4: Drag polar for 100%

5. Conclusion and Recommendations

The initial goal of this experiment was to utilize the open-loop wind tunnel and force balance to experiment and compare the optimal performance of bi-plane airfoils with controlled variables of gap and percent staggered. Issue that occurred to determine the optimal gap was not found and was fixed due to ground effect, thus only aerodynamic characteristics of percent staggered configuration of RAF-15 airfoil was tested. By comparing our data with NACA reports it is important to note that the experiment was done correctly, but it was not as precise as we wanted to be. The bi-plane design was researched more in depth and noticed that the complexity of determining the optimal gap or percent staggered was out of scope. However, it is important to note that the simple addition of another wing would not generate double the lift because of the flow interference from the wings. Also, the Reynolds number calculation was intricate because the Reynolds number was calculated using one chord length, not doubled or the total chord length when staggered. Although two different airfoils were mounted for bi-plane testing in NACA report 70 and NACA report 330 used two Clark-Y airfoils, the NACA report 458 gives collection of data that provides the trend of bi-plane's aerodynamic characteristic relationship of upper and lower airfoil in respect to both airfoils

The results that yielded from the experiment gave more insight to the complexity of determining the optimal gap and percent staggered of bi-plane airfoils. Monoplanes are commonly used today with the improvement in materials and structures, the monoplanes are more efficient by having less drag than bi-planes as well as improvement in L/D for monoplanes.

In conclusion the optimal percent staggered is determined to be that at low angles of attack, the negatively staggered airfoils performs superior to positively staggered airfoils, however at higher angles of attack, positive staggered airfoils had better performance characteristic. This result can be proved with table 3.11, which plots angles of attack 2 degrees and above and the difference in Lift/Drag from positive and negative maximum staggered points.

6. References

Raymer, Daniel P. "Biplane Wings." *Aircraft Design: A Conceptual Approach*. Fifth ed. Reston: AIAA, 2012. 97-99. Print.

Stinton, Darrol. *The Design of the Airplane*. Reston, VA: American Institute of Aeronautics and Astronautics, 2001. Print.

7. Acknowledgements

Matthew Carrico 3D printed the airfoils and Greg Zambrano worked on the pipes to attach the airfoils to force balance.

8. Appendices

8.1. Analysis Procedure

1. Microsoft Excel was used to collect raw data from the wind tunnel laboratory and plotted the aerodynamic properties.
2. Prepared the spreadsheet to input data and immediately plot the data to compare and correct error if error occurred.
3. Formulas and equations were entered into Excel to calculate necessary values.
4. Generated plots and data from the Excel sheet was corrected for foreseen influences, such as wall effect.
5. Compare the plots generated from the experiment to that of theoretical and experimental NACA plots.
6. Computer programs used: LabView and Microsoft Excel and Word

8.2. Sample Computation

$$A = c * s \implies \delta A = \delta c * s + \delta s * c$$

$$SC = c * c * s \implies \delta SC = \delta c * s * c + \delta s * c^2$$

$$q_\infty = \frac{1}{2} \rho V^2 \implies \delta q_\infty = \rho * V * \delta V$$

$$V = \sqrt{\left(\frac{2 * \Delta P}{\rho}\right)} \implies \delta V = \sqrt{\frac{2}{\rho}} * \left(\frac{1}{2}\right) * \left(\Delta P^{-\frac{1}{2}}\right) * \delta \Delta P = \sqrt{\frac{1}{2\rho\Delta P}} \delta \Delta P$$

$$L = F_n \cos(\alpha) - F_a \sin(\alpha)$$

$$\delta L = \cos(\alpha) * \delta F_n - F_n (\sin(\alpha)) \delta \alpha - \sin(\alpha) * \delta F_a - F_a (\cos(\alpha)) \delta \alpha$$

$$\delta L = \sqrt{(\cos^2(\alpha) * \delta F_n^2) + (F_n^2 (\sin^2(\alpha)) \delta \alpha^2) + (\sin^2(\alpha) * \delta F_a^2) + (F_a^2 (\cos^2(\alpha)) \delta \alpha^2)}$$

$$D = F_a \cos(\alpha) + F_n \sin(\alpha)$$

$$\delta D = \cos(\alpha) * \delta F_a - F_a (\sin(\alpha)) \delta \alpha + \sin(\alpha) * \delta F_n + F_n (\cos(\alpha)) \delta \alpha$$

$$\delta D = \sqrt{(\cos^2(\alpha) * \delta F_a^2) + (F_a^2 (\sin^2(\alpha)) \delta \alpha^2) + (\sin^2(\alpha) * \delta F_n^2) + (F_n^2 (\cos^2(\alpha)) \delta \alpha^2)}$$

$$C_L = \frac{L}{q_\infty * A} \implies \delta C_L = \left(\frac{1}{q_\infty * A} \delta L\right) - \left(\frac{L}{q_\infty^2 A} \delta q_\infty\right) - \left(\frac{L}{q_\infty * A^2} \delta A\right)$$

$$\delta C_L = \sqrt{\left(\frac{1}{q_\infty^2 * A^2} \delta L^2\right) + \left(\frac{L^2}{q_\infty^4 A^2} \delta q_\infty^2\right) + \left(\frac{L^2}{q_\infty^2 * A^4} \delta A^2\right)}$$